



## SEISMIC RESTORATION WITH FLEXIBILITY: A NEW METHOD TO MITIGATE DAMAGE TO STRUCTURES DUE TO EARTHQUAKES

S. Igarashi<sup>(1)</sup>, J. Igarashi<sup>(2)</sup>, R. Yakabe<sup>(3)</sup>, T. Kabeyasawa<sup>(4)</sup>

<sup>(1)</sup> Dr. Eng. President, Structural Quality Assurance, Inc., [igarashi.shunichi@sqa.co.jp](mailto:igarashi.shunichi@sqa.co.jp)

<sup>(2)</sup> Head of Management Office, Structural Quality Assurance, Inc., [igarashi.junpei@sqa.co.jp](mailto:igarashi.junpei@sqa.co.jp)

<sup>(3)</sup> Doctor of Science, Structural Quality Assurance, Inc., [yakabe.ryota@sqa.co.jp](mailto:yakabe.ryota@sqa.co.jp)

<sup>(4)</sup> Prof. Emer. Dr. Eng., The University of Tokyo, [kabe@eri.u-tokyo.ac.jp](mailto:kabe@eri.u-tokyo.ac.jp)

### Abstract

In Japanese building code safety alone is required for a major earthquake, serviceability is not. In big cities like Tokyo indirect damage due to the inability to use buildings to affect lives will occur, e.g. crowd avalanches, untreated deaths, energized fires, firestorm, and seismic flooding. The use of facilities is important for securing lives in high density areas. Although the magnitude of ground motion observed in recent years is several times higher than specified in Japanese seismic standards, only a few buildings have collapsed. One-dimensional calculations used in the seismic design may underestimate both the effects of ground motion and the capability of structures. 3D measurements and analyses of the soil-structure system are helpful: a method called Micro Tremor Diagnosis (MTD) is proposed, which measures accelerations at a number of points inside the structure simultaneously and evaluates response characteristics with rms-ratios: central frequency and transfer ratio. MTD is useful for not only measuring main values in seismic resistant design but conducting seismic restoring design based on the 3D modeling of both structure and ground motion.

Forces acting on structures are divided into two types, restoring force toward the stable position and resisting force opposite the relative velocity, e.g. plastic force, viscous force, friction. The work of the resisting force becomes sound, heat, plastic deformation, etc., and cannot be restored. Conventional methods of seismic design, e.g. seismic resistance, seismic isolation, and seismic control, are to use resisting forces to encounter the action of earthquakes, and in principle cause some damage to structures. If we can keep the restoring force after cracking of concrete and minimize the resisting force, we can avoid damage and continue to use the facility after a major earthquake. We call this concept seismic restoration.

A method of reinforcement, placing polyester belts or sheets on structural/nonstructural members or objects with urethane adhesives, has been used for strengthening of structures and taking measures against falling of objects (about 20,000 columns, 1,400 walls, 2400 buildings, 3700 finishing and fixtures, and around 100 infrastructure facilities) in Japan since 2002. Studies on the performance of the buildings and facilities with this method have revealed that (1) damage is rare even after the severe shaking of the Japanese intensity 6 or 7, where many buildings fitting the current seismic code suffered damage to hinder their operation, (2) the vibration from the traffic or earthquakes of intensity 4 to 5 is felt smaller than before, and (3) rolling up main pillars with polyester belt is effective to ensuring safety against collapse of RC buildings. The mechanism of the shaking-reduction by this method was captured by MTD both before and after retrofitting; it is not just to stiffen or to dissipate energy, but to adjust the shape of vibration, so that the structure can contain the energy from the ground within a stable cyclic motion, mainly rotation of each floor. We conclude that reinforcement by the flexible material (polyester) may have realized seismic restoration in recent earthquakes, and call it "Seismic Restoration with Flexibility (SRF)".

Seismic restoring design is proposed to secure serviceability and safety for major earthquakes, using the index  $I_d$  to quantify the degree of damage, and  $I_\alpha$  to evaluate the risk of incident  $\alpha$  to affect life, including  $I_f$ : the risk-index of axial fracture of columns. In the retrofitting of more than 500 buildings in Japan  $I_f$  has already been used as the design index, i.e. main columns are reinforced by polyester belts to secure their axial capacity to support floors without considering increasing the lateral resistance.

*Keywords: Seismic restoration, restoring force, fail-safe, rotation, micro tremor diagnosis*



## 1. Introduction

In Japanese building code safety alone is required for a major earthquake, serviceability is not. That is to say, even if a building can no longer be used, only the life needs to be saved. Response spectra of ground motions observed after the 1995 Great Hanshin-Awaji Earthquake are several times larger than specified as a major earthquake in the current code. Shakings of intensity 7 (the highest grade) on the Japanese scale have been observed in various places, where very few buildings collapsed, while the human and economic damage in recent 25 years (1995-2020) is incomparable to that in previous 25 years until 1995. Recent research has shown that if a direct-type earthquake occurs in Tokyo, crowd avalanches, untreated deaths, energized fires, fire whirlwinds, earthquake floods, etc. will occur and many lives will be lost, and the effects will be long-term. In high density areas, if a building or facility becomes unusable, lives will be endangered. This paper deals with fundamental problems of seismic design and propose new approaches.

## 2. Analysis and measurement of structural response due to ground motion

### 2.1 Conventional model

On the basis of the seismic resistant design is the idea that an earthquake produces a body force in each part of a structure proportional to its mass and ground acceleration. Reality is the opposite. Imagine an actual structure with various 3D shape in the cube drawn with broken lines in Fig. 1 (a). When an earthquake occurs, the ground motion generates contact forces at the boundary of its foundation and soil, e.g. pressure and shear as arrows in Fig. 1 (a). These forces transmit upwards, shaking the structure. On the contrary, seismic resistant design, as drawn in Fig. 1 (b), assumes that an earthquake produces a horizontal acceleration like a lateral gravity, inertial forces proportional to the mass are generated in every part of the structure, they are transmitted to the understory through walls columns and beams down to the foundation, and the surrounding soil yields the reaction called base-shear.

Let us clarify the precondition to treat the ground motion in this way by considering the (vector) equation of motion of a particle “A” constituting the structure as indicated by a black circle in Fig. 1(a):

$$m \frac{d^2 u_0}{dt^2} = f + mg, \quad (1)$$

where  $m$  is the mass of the particle,  $u_0$  is the position vector with respect to (w.r.t.) an inertial frame  $O$ ,  $f$  is the resultant force acting on it except for the gravity, and  $g$  is gravitational acceleration (vector). Rewriting Eq. (1) with the position vector  $u = u_0 - u_{0G}$  w.r.t. a frame “ $G$ ” placed on the ground surface near the structure yields

$$m u'' = f + mg - m u''_{0G} - m(\omega \times (\omega \times u) + 2\omega \times u' + \omega' \times u) = f + mg - m u''_{0G} - m r_{0G}, \quad (2)$$

where  $u_{0G}$  is the position vector of the origin  $G$  of the frame,  $\omega$  is the rotational angular velocity vector representing the rotation of the frame, and dashes imply differentiating components w.r.t. time. The first and the second term on the right side are actual forces, the others ( $m u''_{0G}$  and  $m r_{0G}$ ) are apparent forces due to the motion of the frame  $G$  and the particle A. Neglecting the gravity and apparent forces except that due the translational acceleration in a horizontal direction  $x$ , and writing only  $x$ -component of the vectors in Eq. (2),

$$m u''_x = f_x - m u''_{0Gx}. \quad (3)$$

Assuming  $f_x = -k u_x - c u'_x$  in Eq. (3), where  $k$  is the spring coefficient, and  $c$  is the viscosity coefficient,

$$m u''_x + k u_x + c u'_x = -m u''_{0Gx}. \quad (4)$$

This equation and similar ones for multiple particles as shown in Fig. 1(b) are widely used for the response analysis of earthquake resistant design, and the basis of the idea that an earthquake produces a horizontal acceleration. As shown in the above process of deriving Eq. (4) from Eq. (1) this model requires the conditions that (1) the ground be a rigid plane and move only horizontally without rotation, (2) the connection between



the ground and the structure be rigid, (3) each layer of the structure can be modeled as a particle, and (4) displacement be small and one directional. Even if three-dimensionality is aside, the difference between this model and the actual response of a structure will increase as the level (PGA or rms) of the ground motion does: when the nonlinearity of soil and structure becomes obvious, the frame G itself loses ground.

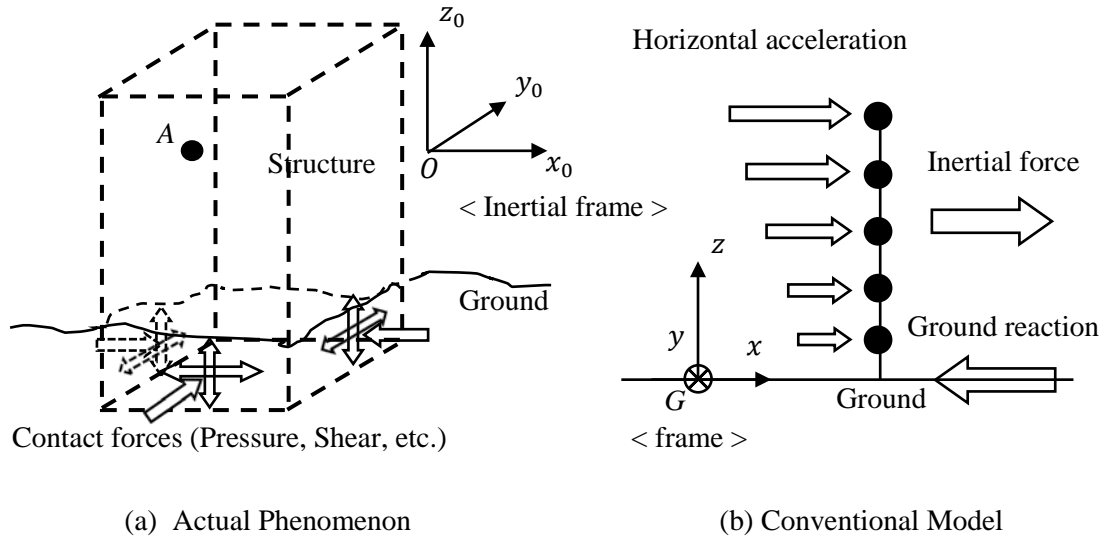


Fig. 1 Actual phenomenon and conventional model

## 2.2 Observed ground motion and damage

The strong motion observation had been considered important for rationalizing seismic design, since the ground acceleration is the input to the structure in Eq. (4). Before 1995 researchers had compared the PGA of a newly observed strong motion record with the design value, i.e. 0.3 to 0.4G ( $G=9.8m/s^2$ ) in Japanese code, and the media had also followed up. In the 1993 Kushiro-Oki earthquake PGA of 0.9G was recorded at the meteorological observatory in Kushiro, and immediately announced. The surprised media and researchers thronged there. Afterwards, there have been observed PGA several times larger than the design value, one after another, e.g. 0.8G at Kobe in the 1995 Great Hanshin-Awaji Earthquake, 2.5G at Kawaguchi-cho in the 2004 Niigata Chuetsu Earthquake, and 4.1G at Ichinoseki-shi in the 2008 Iwate-Miyagi Inland Earthquake (registered in Guinness Book of Records). However, no building collapsed around the observatories. The ratio of the collapsed building is only a few percent, even in the areas of Japanese intensity 7 of the above earthquakes, except for pilotis buildings. Recently, no one cares about the big gap between the observed PGA or response spectrum with the design level.

The Tokyo-Kantei, a real estate datum company, published a report on its website, investigating the damage rate of condominium buildings in Kumamoto city after the 2016 Kumamoto Earthquake, and comparing it with previous big earthquakes. The rates of no-damage are 51% out of 5261 buildings in Hyogo Prefecture after the 1995 Great Hanshin-Awaji Earthquake, 50.5% out of 1460 in Miyagi Prefecture after the 2011 Great East Japan Earthquake, and 24% out of 722 in Kumamoto city after the 2016 Kumamoto Earthquake. The report concluded that the Kumamoto Earthquake had recorded the smallest and worst rate of no-damage (70 percent or more suffered a certain damage). The numbers of collapsed condominium buildings are only one in the Kumamoto Earthquake, and none in the other two. Engineers and researchers tend to focus on the rate of severe damage. Owners are interested in the rate of no-damage, which has not been improved since the 1995 Kobe Earthquake. It is a social demand to reduce damage to buildings and ensure continuity of use.

## 2.3 Three-dimensional model

The configuration and deformation of a structure with columns, beams and slabs, e.g. a building and a railway viaduct, can be represented by layers, axes and interlayer deformations as shown in Fig. 2.

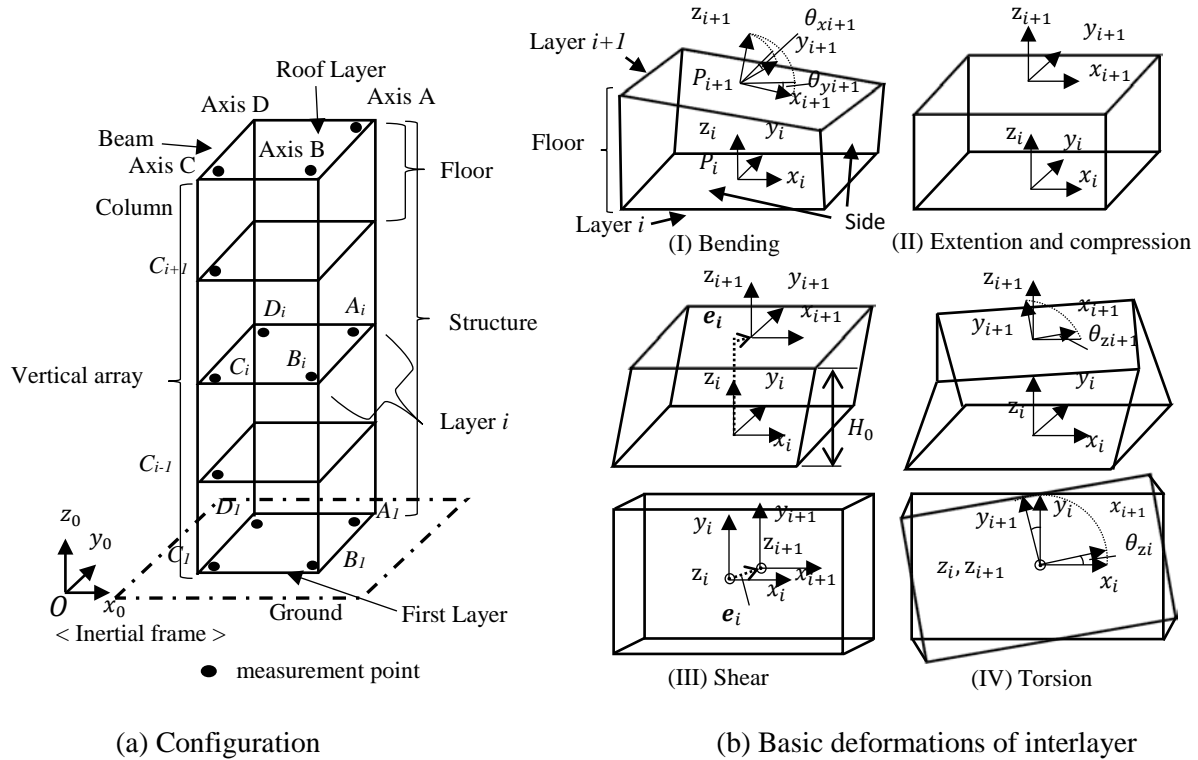


Fig. 2 Three-dimensional model of a structure with layers and axes

Assuming a layer is rigid, and its displacement and rotational angle are small, they can be calculated by the displacements measured in 3 points on the layer using the relation

$$a(t) \approx p(t) + \theta(t) \times r_a, \quad (5)$$

where  $a(t)$  is the displacement of point A fixed on the layer,  $r_a$  is its position vector,  $p(t)$  is that of the origin of the frame with  $x$  and  $y$  axes embedded in the layer, and  $\theta(t)$  is its rotational angle (vector); their  $x$ -components

$$\theta_x(t) = \frac{a_z(t)(x_c - x_b) + b_z(t)(x_a - x_c) + c_z(t)(x_b - x_a)}{y_a(x_c - x_b) + y_b(x_a - x_c) + y_c(x_b - x_a)}, \quad (6)$$

$$p_x(t) = \frac{a_x(t) + b_x(t) + c_x(t) + \theta_z(t)(y_a + y_b + y_c)}{3}, \quad (7)$$

where  $a_k(t)$ ,  $b_k(t)$ ,  $c_k(t)$  is the  $k$ -component ( $k=x, y, z$ ) of the displacement of point A, B, and C placed on the layer, respectively, whose coordinates are  $A(x_a, y_a, 0)$ ,  $B(x_b, y_b, 0)$ ,  $C(x_c, y_c, 0)$ , and where the  $z$ -component of  $\theta(t)$

$$\theta_z(t) = \frac{a_x(t) - b_x(t)}{y_b - y_a} = \frac{b_x(t) - c_x(t)}{y_c - y_b} = \frac{c_x(t) - a_x(t)}{y_a - y_c} = \frac{a_y(t) - b_y(t)}{x_a - x_b} = \frac{b_y(t) - c_y(t)}{x_b - x_c} = \frac{c_y(t) - a_y(t)}{x_c - x_a}, \quad (8)$$

where subscripts  $i$  or  $i+1$  in Fig. 2 (b) are omitted. The  $k$ -component of rotational angular velocity vector  $\omega_k$  in Eq.(2) is obtained by differentiating  $\theta_k$  w.r.t. time, i.e.

$$\omega_k(t) = \theta_k'(t). \quad (9)$$

Quantities of interlayer deformations in Fig. 2 (b), e.g. interlayer drift ( $e_i$ ), axial strain, and curvature of an axis, can be calculated from the displacements and rotations and the geometry of each layer.



## 2.4 Micro Tremor Diagnosis (MTD)

Every structure on the ground always vibrates due to the ground motion with an amplitude of several microns (micro tremor). Its energy-source is a tide, traffic, etc. As a structure has been vibrating since its completion, its micro tremor becomes to exhibit the fundamental mode of vibration. If we assume that, when an earthquake occurs, a structure amplifies its fundamental mode to a certain extent, then we can obtain the structural vibratory characteristics and predict its response due to ground motion by (1) measuring the micro tremor as the acceleration time histories simultaneously at measurement points located in the structure (Fig. 2 (a)), (2) calculating the time history of the jerk, velocity, displacement, and the physical quantity of interest, e.g. interlayer drift, rotation, strain etc., from the acceleration time history of each point, (3) taking the root-mean-square (rms) ratio between time histories, and (4) estimating design indices, e.g. the base shear factor at yielding, assuming that the rms-ratios are conserved until yielding.

Let  $y(t)$  be a time history with duration  $[0, t_0]$ , rms of  $y(t)$ :

$$\sigma_y \equiv \sqrt{\frac{1}{t_0} \int_0^{t_0} y^2(t) dt} . \quad (10)$$

Its central frequency

$$\omega_{cy} \equiv \frac{2\pi}{T_{cy}} = \frac{\sigma_{y'}}{\sigma_y} , \quad (11)$$

where  $T_{cy}$  is the central period and  $\sigma_{y'}$  denotes the rms of  $y'(t)=dy(t)/dt$ . If  $y(t)$  is a segment of a stationary Gaussian process,  $\omega_{cy}$  is its mean frequency of zero crossing.

Considering the shear force between layers is the product of acceleration and its mass, the interlayer shear force distribution factor

$$A_{ikm} \equiv \frac{\sum_{j=i}^n m_j \sigma_{ajk} / \sum_{j=i}^n m_j}{\sum_{j=1}^n m_j \sigma_{ajk} / \sum_{j=1}^n m_j} , \quad (12)$$

and the acceleration amplification factor

$$B_{a1k} \equiv \left( \sum_{j=1}^n \sigma_{ajk} m_j / \sum_{j=1}^n m_j \right) / \sigma_{a1k} = \sum_{j=1}^n h_{a:ajk} m_j / \sum_{j=1}^n m_j , \quad (13)$$

where  $\sigma_{a:jk}$  is the rms of the  $k$ -component of acceleration of the  $j$ 'th layer  $a_{jk}(t)$ , and  $m_j$  is its mass, and

$$h_{a:aik} \equiv \frac{\sigma_{aik}}{\sigma_{a1k}} . \quad (14)$$

If we assume that above factors and the ratio between the rms of the interlayer drift  $e_{ik}(t) = d_{i+1k}(t) - d_{ik}(t)$  and the base acceleration  $a_{1k}(t)$  are conserved until yielding i.e.

$$h_{a:eik} \equiv \frac{\sigma_{eik}}{\sigma_{a1k}} = const. , \quad (15)$$

where  $d_{ik}(t)$  is the  $k$ -component of the displacement of the  $i$ 'th layer, then we can estimate the base-shear factor at yielding of the  $i$ 'th layer



$$C_{bYikm} = B_{a1k} \frac{e_{Yik}}{h_{a;eik} \cdot G} = B_{a1k} \frac{R_{Yik} H_{0ik}}{h_{a;eik} \cdot G}, \quad (16)$$

where  $e_{Yik}$  is the interlayer drift at yielding,  $R_{Yik} = e_{Yik} / H_{0ik}$  is its angle,  $H_{0ik}$  is the floor height, and  $G$  is the gravitational acceleration constant ( $9.8m/s^2$ ). Generalizing Eq. (14) and (15), we can define coefficients to express the shape of vibration due to ground motion from micro tremors to earthquakes called transfer ratios:

$$h_{x;y} \equiv \frac{\sigma_y}{\sigma_x}, \quad (17)$$

Where  $\sigma_y$  is the rms of a time history  $y(t)$ , and  $\sigma_x$  is that of the reference time history  $x(t)$  in the 1st layer. The suffixes of  $x(t)$  and  $y(t)$  are written as the suffix of  $h$  after  $x$  and  $y$  in the same size, omitting the same ones.

### 3. Seismic Restoration with Flexibility

#### 3.1 Seismic restoration

Our challenge is how to build a structure that can be used after severe ground motions exceeding 1G. There is a testimony of a woman who actually experienced such a ground motion in Mashiki town, Kumamoto city during the 2016 Kumamoto Earthquake. In a program called NHK Special aired on April 9, 2017 she said: “It was like a house box shaken vertically. I’m like a ping-pong ball because I can’t do anything. The living room and the like broke like twisting. As the wall came off more and more, I was able to see inside with the light outside. Anyway, my body just moves in the direction of being shaken.” Her wooden two-story house was completely destroyed with the first floor collapsed. While displacement is small, each part of a structure keeps elasticity and vibrates around its stable position. When the displacement exceeds the elasticity limit, cracks in concrete widen and rebars yield. In wooden structures, joints open accompanying yielding of hardware. In each part of the structure appear resisting forces, e.g. plastic force, viscous force, frictional force. They just resist the relative motion, consume the kinematic energy into sound and heat, and leave plastic deformation. As she said “my body just moves in the direction of being shaken.” It is impossible to restore the original configuration once the resisting force did its work: we cannot trace back every path of the inelastic motion.

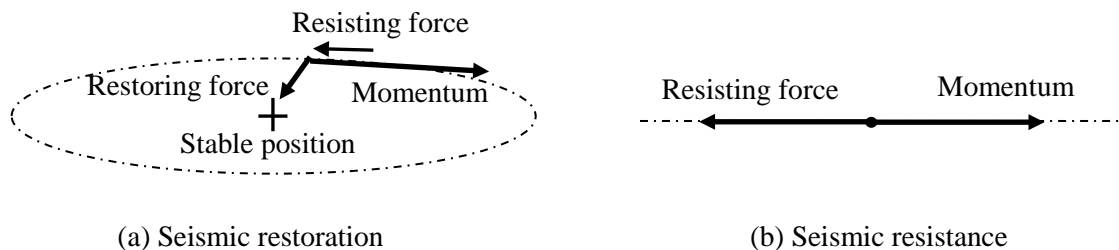


Fig. 3—Seismic restoration vs resistance

Fig. 3 shows the concept of seismic restoration versus resistance. An earthquake ground motion gives momentum (product of mass and velocity) to each part of a structure. The seismic restoration changes the direction of the momentum by restoring force and contains the energy from the ground in the motion around the stable position (Fig. 3 (a)). On the contrary, conventional concepts, e.g. the seismic resistant, isolation, vibration control, try to make the resisting force encounter the momentum head on (Fig. 3 (b)). If the resisting force is insufficient, then the structure breaks down. Otherwise, the motion may stop in a short time at the expense of irreversible deformation: damage. A key to seismic restoration is to maintain the restoring force during a major earthquake, i.e. beyond the elasticity limit of concrete and steel.

Two types of deformation of a story with 4 columns due to the rotation of the top of the columns around their stable positions are illustrated in Fig. 4; on the left is the special case where the phase of the rotation of each column is the same (Fig. 4 (a)), and every part of the upper layer is moving circularly relative to the lower



layer; on the right (Fig. 4 (b)) is a general case where the phases differ, every point of the upper layer moves with different radius and phase, the center is rotating around the z-axis, the floor (interlayer) experiences torsion, and the side planes are twisted. Other keys to seismic restoration are that (1) columns should keep restoring force three dimensionally, (2) walls should maintain structural unity to twisting, and (3) joints should function under 3D motion like an arm or shoulder joint.

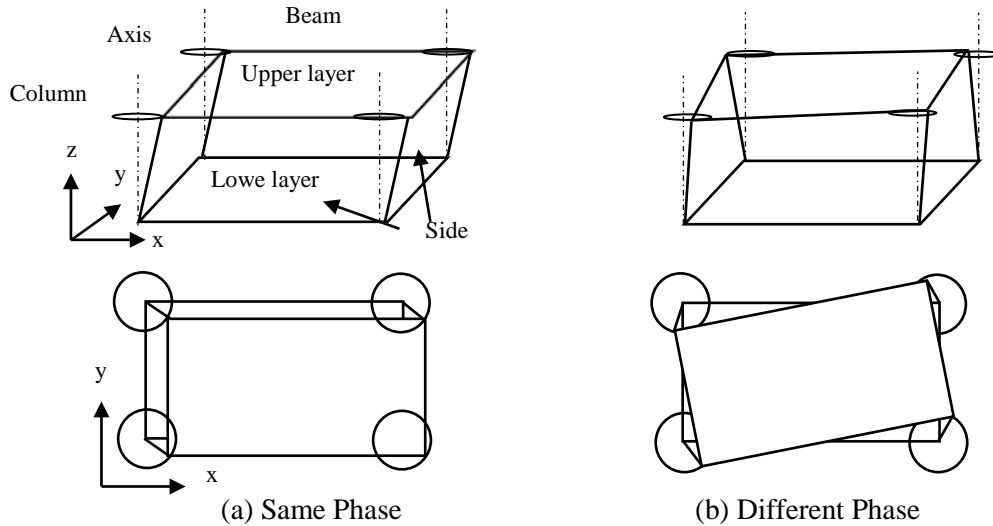


Fig. 4–Deformation of a 4-column story

The elements of seismic resistant design, e.g. walls, steel braces, joint hardware and dampers, are fixed to the structure to exert resisting force in one direction. However, the actual ground motion requires the device and its mounting part to move in a direction that fluctuates three-dimensionally, they can come off or break as she experienced: “The living room and the like broke like twisting. As the wall came off more and more, I was able to see inside with the light outside.” In the 2016 Kumamoto Earthquake, there have been many reports of seismic isolation and damping devices themselves being damaged, or mounting parts being destroyed.

### 3.2 Reinforcement by flexible material

A method of reinforcement (Photo 1), placing polyester belts or sheets on structural/nonstructural members or objects with urethane adhesive, has been used for strengthening structures and taking measures against falling of objects in Japan since 2002: about 20,000 columns, 1,400 walls, 2400 buildings, 3700 finishing/fixtures and around 100 infrastructure facilities.

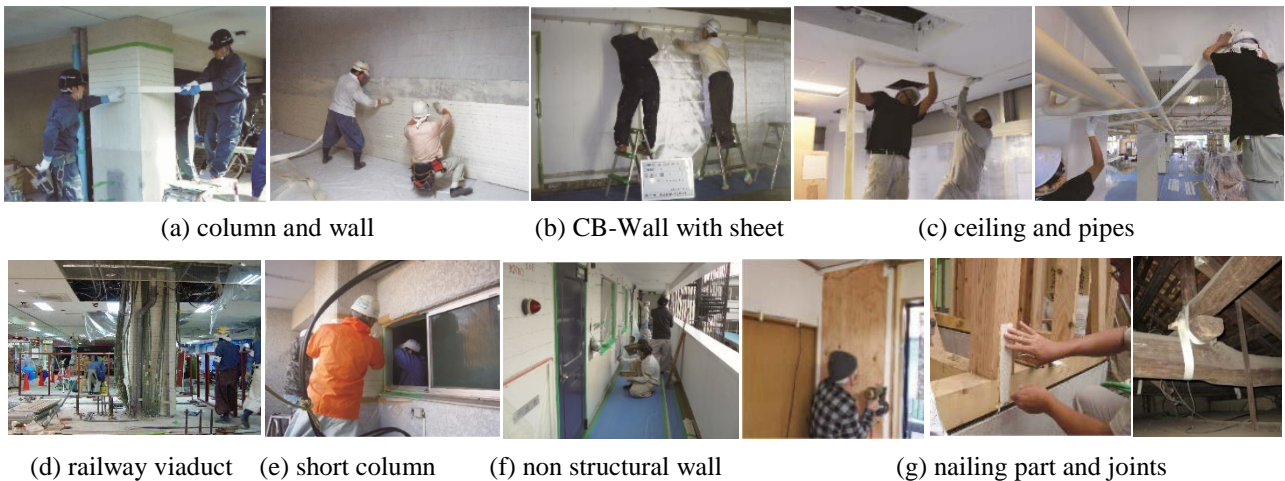


Photo 1– Reinforcement by polyester belts or sheets



The flexible material (polyester sheet or belt) is almost elastic up to 10% strain with the effect to (1) give restoring force to concrete crack widening and gapping, (2) prevent the cover concrete from falling off, (3) increase the compression-failure strain of concrete due to axial load and/or bending, (4) support floors even after the inside concrete were smashed into pieces by a great number of cyclic loadings. Static component tests and a shake table frame test verified that this method can give a remarkable restoration even to a short column under high varying axial load and many cycles of lateral loadings [1, 2].

In an office building near Tokyo the completion of seismic renovation with this method in 2005 for a main column in each floor settled the traffic vibration. In another building in the Tokyo bay area tenant people reported that the shaking of Japanese seismic intensity 4 in November 2013 was felt much smaller after the renovation. There was a total of 462 (301 non-wooden, 154 wooden, 7 infrastructure) facilities reinforced by this method in the area whose seismic intensity is 5 or more, 60 buildings were in the area of intensity 6 or more of the 2011 Great East Japan Earthquake. Investigation by telephone, facsimile, visit, etc., revealed that all of them has been functional right after the earthquake without any damage even in the finishing. Many owners replied with gratuity that the shaking was small. In the 2016 Kumamoto earthquake, despite serious damage to new buildings and retrofitted ones by conventional methods in the same area of Kumamoto city, 7 buildings with this method were no damage.



View Columns with polyester belts

Photo 2—A building near Sendai Station

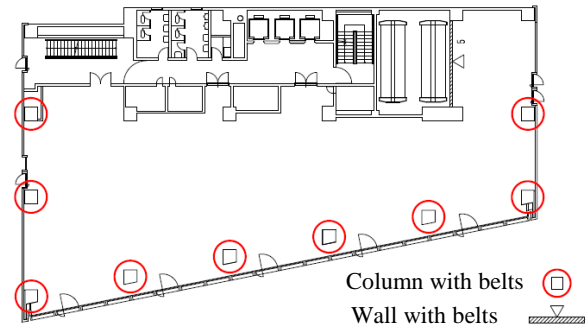
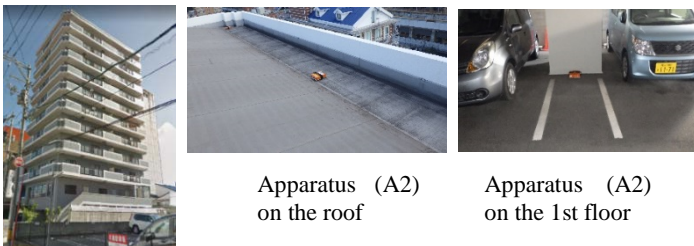


Fig. 5—Plan

A 9-story building near Sendai station (Photo 2) suffered severe damage, e.g. many big cracks on walls and columns, from the 2008 Iwate-Miyagi Inland Earthquake. Fig. 5 shows the plan. This is a typical eccentric building with walls located on one side. Conventional retrofitting would be to put bracings on the other side, so that the eccentricity could be canceled by their rigidity. Contrarily, we covered independent columns and a wall with polyester belts as marked in Fig. 5. According to the manager who were in the basement of the building and checked damage right after the 2011 Great East Japan Earthquake, there was almost no damage, not a crack in the finishing, as if there had been no earthquake at all; he was surprised remembering the severe damage in the 2008 earthquake. While other buildings near the Sendai station, and the station itself had to close more than one month, since the 4th day after the earthquake, this building had operated as a temporary department store, where thousands of people gathered to buy daily necessities.

### 3.3 Micro tremor diagnosis both before and after reinforcement by polyester belts

An 11-story condominium pilotis building (completion 1995, SRC) was reinforced by polyester belts in 2017. Only two independent columns in the first floor were covered with polyester belts. Micro tremor diagnosis (MTD) were carried out both before and after the reinforcement.



Apparatus (A2) on the roof Apparatus (A2) on the 1st floor

Photo 3—A pilotis building and MTD apparatus

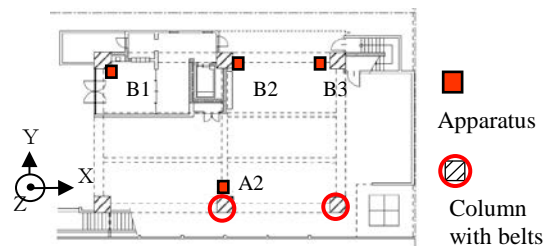


Fig. 6—Location of reinforced columns and apparatuses





Table 1–Transfer ratios before and after reinforcement

floor	Before			After			Bef./Aft.		
	X	Y	Z	X	Y	Z	X	Y	Z
RP	0.43	0.77	0.13	0.05	0.02	0.10	0.11	0.03	0.79
R(12)	12.7	7.94	1.47	4.80	3.46	1.04	0.38	0.44	0.71
11				2.35	2.63	0.99			
10				2.28	2.30	1.03			
9				1.96	2.11	1.03			
8	2.66	3.55	1.22	1.89	1.99	0.97	0.71	0.56	0.80
7				1.91	1.80	0.97			
6				1.84	1.58	0.96			
5				1.60	1.47	1.06			
4	1.54	2.10	1.09	1.42	1.28	1.06	0.92	0.61	0.97
3				1.15	1.11	1.04			
1	1.00	1.00	1.00	1.00	1.00	1.00	1.00	1.00	1.00

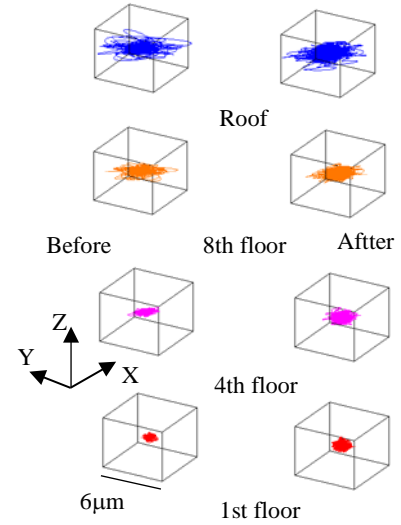


Fig. 7–Orbits of B2 array

Fig. 6 shows the location of the columns and apparatuses of MTD in the 1st floor. Two vertical arrays were formed near B2 and B3 columns. On the roof 2 apparatuses were added near B1 and B3 column to measure its rotation and inclination. Only 4 apparatuses were available in the measurement before reinforcement. Therefore, the vertical arrays were on the 1<sup>st</sup>, 4<sup>th</sup>, 8<sup>th</sup> floor and the roof. After reinforcement we used 12 apparatus and placed them on each floor except for the 2<sup>nd</sup> where we could not enter. We recorded acceleration for 5 minutes in the before-reinforcement measurement simultaneously, for 10 minutes in the after-reinforcement. The time-histories were divided into 3 parts of 2 minutes long, processed with a 10 Hz high cut-off filter and a 0.2-Hz low cut-off filter (4th Butterworth). Their velocity and displacement were calculated by the numerical integration with linear acceleration method. The quantity and indices defined in sections 2.3 and 2.4, e.g. central period, interlayer shear force distribution factor, of each part were calculated and their means and standard deviations were obtained. Fig. 7 shows orbits of a typical part of both before and after reinforcement. Table 1 lists the transfer ratios (TR) of displacement, i.e. in Eq. (17)  $y(t)=d_{ik}(t)$ ,  $x(t)=d_{ik}(t)$ ,  $i=1,3, \dots, 12$ ,  $k=x,y,z$ , where  $d_{ik}(t)$  is the  $k$ -component of the displacement of the  $i$ 'th floor. The TR of the after-reinforcement decrease to around 40% of the before-reinforcement. On the top line (RP) are the TR of the displacement  $p_{12k}(t)$  and rotational angle  $\theta_{12k}(t)$  of the roof layer calculated by Eq. (6) to (8), where the denominator of Eq. (17):  $x=(d^2_{1x}(t)+d^2_{1y}(t))^{1/2}$ , and the decrease of the inclination of the roof (10% around the  $x$ -axis, 3% around the  $y$ -axis) is remarkable. This can be interpreted that reinforcement by the flexible material has adjusted the vibration of the building so that the amplification of the displacement and inclination be small.

Table 2–Interlayer shear force distribution factor, Central Period and Base-shear factor at the yielding

Floor	$A_{ikm}$					Cal. T	$T_{cdk}$ [sec]				$C_{bYikm}$				
	Cal. $A_i$	B2		B3			B2		B3		B2		B3		
		X	Y	X	Y		X	Y	X	Y	X	Y	X	Y	
11	2.39	2.25	1.94	1.62	1.60	0.6	0.68	0.81	0.59	0.60	0.19	0.35	0.50	0.85	
10	1.95	1.80	1.65	1.54	1.50		0.72	0.80	0.67	0.60	0.37	0.52	0.39	1.11	
9	1.73	1.60	1.49	1.48	1.41		0.70	0.81	0.59	0.61	0.51	0.65	0.34	1.39	
8	1.58	1.47	1.38	1.40	1.33		0.73	0.84	0.60	0.63	0.51	0.70	0.58	1.32	
7	1.46	1.37	1.30	1.34	1.27		0.81	0.84	0.69	0.63	0.40	0.75	0.53	1.26	
6	1.37	1.30	1.24	1.28	1.22		0.91	0.85	0.66	0.67	0.38	0.64	0.45	1.12	
5	1.28	1.24	1.19	1.22	1.17		0.93	0.88	1.10	0.70	0.32	0.64	0.24	0.83	
4	1.21	1.18	1.14	1.18	1.14		1.02	0.92	0.81	0.73	0.38	0.64	0.23	0.73	
3	1.14	1.12	1.10	1.12	1.10		0.99	0.93	0.76	0.77	0.49	0.82	0.49	1.17	
2	1.08	1.06	1.05	1.07	1.06					0.85	0.89			0.87	1.26
1	1.00	1.00	1.00	1.00	1.00					1.23	1.41	1.13	1.10		0.70



Table 2 shows the interlayer shear force distribution factor  $A_{ikm}$  (Eq. (12)), central period  $T_{cdk}$  (Eq. (11)), and the base-shear factor at the yielding  $C_{bYikm}$  (Eq. (16)), along with the numbers calculated by the Japanese design-guideline;

$$A_i = 1 + \left( \frac{1}{\sqrt{\alpha_i}} - \alpha_i \right) \frac{2T}{1 + 3T}, \quad T = 0.02h, \quad \alpha_i = \sum_{j=i}^n m_j / \sum_{j=1}^n m_j, \quad (18)$$

where  $m_j$  is the mass of the  $j$ 'th floor, and  $h = 29.1m$  is the height of the building. The measured  $A_{ikm}$  of upper floors are smaller than the calculation ( $A_i$ ), reflecting that this building is a pilotis and does not amplify the ground motion so much as the ordinary buildings do. The measured  $T_{cdk}$  are similar to the calculated  $T$  in both directions except for 1<sup>st</sup> layer and 3<sup>rd</sup> to 5<sup>th</sup> layer. In the base shear factors  $C_{bYikm}$  those of  $y$ -direction are greater than those of  $x$ -direction except B2 of 11<sup>th</sup> floor. There are walls between A2 and B2 in the  $y$ -direction from the 2<sup>nd</sup> floor up to the 10<sup>th</sup>. In the 11<sup>th</sup> floor the wall has been removed. The values of 4<sup>th</sup> and 5<sup>th</sup> floors are smaller than the others. The designer of this building remembers that it rained so heavily that the concrete placing was suspended and rescheduled one week later when 4<sup>th</sup> or 5<sup>th</sup> floor was constructed. There might be some construction joints or defect in these floors. In this case measured base shear factors are consistent with building reality. From 2017 until 2020, MTD has been carried out for 11 buildings, where similar results have been obtained, e.g. the measured factors in a new 12-story building match or differ reasonably to those in the structural calculation sheet; the TR changed into around 70% of the before- reinforcement value in before-under-and-after reinforcement measurements of a 9-story building.

Table 3–Transfer Ratios of the center and Apparent accelerations at B1 on the roof

Transfer Ratios (TR)						Apparent accelerations at B1 [ $\mu m / s^2$ ]								
Translation			Rotational Angle			Translation $u''_{OG}$			Rotation $r_{OG}$			Rot. / Trans.		
X	Y	Z	X	Y	Z	X	Y	Z	X	Y	Z	X	Y	Z
2.28	2.47	0.94	1.04	0.92	3.21	64.7	72.6	39.3	145.4	168.6	52.7	2.25	2.32	1.34

The left side of Table 3 shows TR of the translation ( $h_{d;d12k}$ ) and rotational angle ( $h_{\theta;\theta12k}$ ) of the center of the roof after reinforcement. The horizontal ( $x$  and  $y$ ) translations amplified around twice, while the vertical displacement and rotational angle around the horizontal axes is not. The rotation around the vertical ( $Z$ ) axis is amplified more than three times. This illustrates that this building, after reinforcement, contains a significant part of the energy of ground motion as the rotation around the vertical axis.

The right side of Table 3 shows the rms of the apparent accelerations at point B1 on the roof defined in Eq. (2) as  $u''_{OG}$  and  $r_{OG}$ , and calculated from the measured time history using Eq (6) to (9) with frame G on the 1<sup>st</sup> floor. The horizontal rotations of the 1<sup>st</sup> floor are found to bring the apparent acceleration to the roof more than twice as much as the translations do. If we assume that the motion of this building is amplified by an earthquake conserving this mode, and the movement of the ground and the 1<sup>st</sup> floor is similar, then the effect of earthquakes may be underestimated by a third if we neglect apparent acceleration due to the rotation of the 1<sup>st</sup> floor, i.e. ground. 3D modeling of both structure and ground motion is important to seismic design.

## 4. Seismic restoring design

### 4.1 Safety

Seismic restoring design targets both safety and functionality during and after a major earthquake. If a structure is usable, then it must be safe. The safety is jeopardized only when the premise and method to check the serviceability breaks down: the safety should be secured by the fail-safe device designed and installed in case of emergency. Let us imagine events where life is endangered by a structure, e.g. (1) finishing, facility, furniture, etc. tumbles and bumps into people, (2) the structure falls as a whole suddenly, (3) some joints separate, vertical members or beams fall, making the internal space decrease and people be caught, (4) a column buckles, making a part of the structure collapse, (5) people jump down as escaping and/or collide



mutually, (6) the intoxication by a gas leak, an electric shock, etc. occurs, (7) the burn by a fire, a dyspnea, etc. happens, and (8) incidents caused by the inability to use the facility, e.g. economy class syndrome, untreated deaths, electricity fire, occur.

Since an event belonging to (1) to (4) is where things fall or break, its risk can be quantified by the index

$$I_{\alpha} \equiv \max_p (i_{\alpha p}) = \max_p \left( \frac{q_{\alpha p}}{r_{\alpha p}} \right), \quad (19)$$

where  $q_{\alpha p}$  is the magnitude of the driving force of the event  $\alpha$  due to the major earthquake,  $r_{\alpha p}$  is that of the restoring force mobilized by the fail-safe device installed to encounter the event, and  $p$  represents the location of the event. For the first category, i.e. tumbling of finishing or objects ( $\alpha=t$  in Eq. (19)), reinforcement by polyester belts has been used as the fail-safe device as shown in Photo 1 (c). Structural failure in a narrow sense is caused by an event in the categories (2), (3) and/or (4). Considering, in low-rise to mid-rise Reinforced Concrete (RC) buildings in Japan, the risk of (2) and (3) can be by far smaller than that of (4), i.e. the index of axial fracture of columns:

$$I_f \equiv \max_p (i_{fp}) = \max_p \left( \frac{N_{sp}}{N_{up}} \right) \quad (20)$$

can determine the risk, where  $N_{sp}$  is the magnitude of the maximum axial load of the column  $p$  during the earthquake, and  $N_{up}$  is the capacity of the column against its axial crush. Model tests and theoretical study proved that rolling up a column with polyester belts acts as the safety device with the capacity

$$N_{up} = \frac{(1 + \sin \phi)}{(1 - \sin \phi)} \frac{\pi b D}{(b + D)} t E_f \varepsilon_{fu}, \quad (21)$$

where  $\phi$  is the friction angle (40 degree) of the crashed concrete,  $b$  and  $D$  is the width and depth of the column  $p$ , and  $\varepsilon_{fu}$ ,  $t$  and  $E_f$  is the maximum strain, thickness and Yong's modulus of the belt, respectively. Eq. (21) is derived by a physical model (Mohr-Coulomb's failure criterion) where the concrete was smashed into pieces like sand and the surrounding polyester belts confine it.

$I_f$  in Eq. (20) has been used as the design index in the retrofitting of more than 500 buildings since 2003: main columns of a building are reinforced by polyester belts to secure their axial capacity without considering to increase the lateral resistance. This method of retrofitting is called "Axial Reinforcement (AR)". No damage to these buildings has been reported in the 2011 Great East Japan Earthquake, 2016 Kumamoto Earthquake, and others. Saijo City, Ehime Prefecture, decided to use AR for all municipal public facilities, and completed reinforcement of 45 buildings from 2008 to 2018, including 28 school buildings. The cost and the construction period of AR were a fraction of those of the conventional method, e.g. steel bracing.

#### 4.2 Serviceability

Rebars in RC and joint hardware in wooden structures accumulate permanent deformation under cyclic loading beyond the elasticity limit, damaging concrete and wood at their contact surface. As a result, the stable configuration of the structure will change. A damage mitigating device should maintain restoring force after these microscopic and finite change beyond the elasticity limit, whose efficiency can be evaluated by measuring the work

$$w_{fp} \equiv \int_0^{t_l} f_p \cdot \frac{ds_p}{dt} dt \quad (22)$$

done by resisting force  $f_p$  in a multi-dimensional cyclic loading test of a member  $p$  with the device, where  $t_l$  is the time when the residual deformation reaches the design limit, e.g. 1% , and  $ds_p$  is the incremental trail vector of the point of action of the force vector  $f_p$  in time increment  $dt$ . This work depends on the trail. We have to



decide the test method, e.g. to move the capital so as to draw a circle w.r.t. the pedestal of the member and gradually increase the radius of the circle.

If we can estimate the work “ $w_{Ep}$ ” done to the member “ $p$ ” of a part “ $c$ ” of a structure during the major earthquake “ $E$ ”, then the indices

$$I_{duEc} \equiv \underset{p \in c}{\text{Max}} \left( \frac{w_{Ep}}{w_{lp}} \right) \quad \text{and} \quad I_{dmEc} \equiv \underset{p \in c}{\text{Average}} \left( \frac{w_{Ep}}{w_{lp}} \right) \quad (23)$$

can express the degree of damage of the part. In the 1/3 scale model test of eccentric pilotis 6-story RC buildings on a shaking table, where one building is reinforced by polyester belts and sheets, the other one is bear RC, the work of the bear RC building calculated by Eq. (22) until collapsing was about 1/5 of the work done to the reinforced building. The residual drift angle of the reinforced one after receiving 3 major ground motions, including the Takatori-record in the 1995 Great Hanshin-Awaji Earthquake was negligible and after 7 ground motions about 5% [2].

#### 4.3 Design procedure

Seismic restoring design is based on the normal design method and adds the steps of ensuring usability and safety against a major earthquake: it has the step to (1) determine the size, configuration according to legal, architectural, functional, and financial requirements and conditions tentatively, (2) check the serviceability and safety against service load and environmental conditions except for earthquakes, (3) put damage-mitigating devices for both structural and nonstructural members so that the damage due to a major earthquake should not affect the serviceability, (4) install appropriate countermeasures against each incident that endangers lives and check the risk, and (5) make sure if the risk is acceptable, otherwise reconsider from the beginning.

The 3D linear model with layers and axes illustrated in Fig. 2 can be used to calculate the response and estimate the work done to a part of the structure due to the design earthquake. Measuring micro tremor and calculating design factors (MTD) of a new building will help to verify the model and check the quality of construction. Using flexible material like polyester belts and sheets will serve in damage mitigating and fail-safe for incidents where things fall or break. The other events to affect life should be taken care of individually. If a large-scale facility is to be located in a densely populated area, it will not be possible to accurately predict the appearance and risk of events after a major earthquake. In such a case, it is important to consider abandoning the construction itself.

### 5. Conclusion

We have arrived at the conclusion that (1) Micro Tremor Diagnosis (MTD) is useful for not only measuring key values in seismic resistant design, e.g. base-shear factor at yielding, but conducting seismic restoring desing based on the 3D modeling of both structure and ground motion, (2) a reinforcement method, placing flexible material (polyester belts or sheets) on main structural/non-structural members in a constructed facility, avoided damage and made it usable after recent earthquakes, and (3) this method can keep the restoring force of members after cracking of concrete, minimize the resisting force and adjust the shape of vibration, so that the structure may contain the energy from the ground within a stable cyclic motion, mainly rotation of each floor around the vertical axis. We have called this mechanism seismic restoration and this method Seismic Restoration with Flexibility (SRF).

### 6. References

- [1] Kabeyasawa T, Tasai A, Igarashi S (2004): Test and analysis of reinforced concrete columns strengthened with polyester sheet. *13th World Conference on Earthquake Engineering* Vancouver, B.C., Canada.
- [2] Kabeyasawa T, Igarashi S, Kim Y (2004): Shaking table test of reinforced concrete frames for verification of seismic strengthening with polyester sheet. *13th World Conference on Earthquake Engineering* Vancouver, B.C., Canada.